Jordan Journal of Civil Engineering, Volume **17**, No. **1**, **2023**
DOI: https://doi.org/10.14525/JJCE.v17i1.03

Nonlinear Finite Element Analysis of High-strength Reinforced Concrete Beams with Severely Disturbed Regions

Qasim M. Shakir [1)*], ***Yahya M. Al-Sahlawi*** [1)], ***Baneen B. Abd*** [1)] ***and Sarah A. Hamad*** [1)]

[1)] Civil Engineering Department, Faculty of Engineering, University of Kufa, Najaf, Iraq. * Corresponding Author.

ABSTRACT

The inclusion of D-regions within a reinforced-concrete member may affect largely the general behavior of the structure. Different techniques and approaches were proposed to control the behaviour of D-regions, such as the shear-friction approach and the STM model. Such proposals may not be applicable for all types of D-regions. The current work presents a nonlinear finite element model using the ANSYS software, that is adopted to study three types of D-regions, which are dapped ends, deep beams with openings and beams with loaded openings.

The results revealed that the proposed FE model predicted adequately the effects of the inclusion of D-regions in RC beams. It is found that reducing the hanger or the nib reinforcement of a dapped end by 25% resulted in reducing capacity by 15% and 32%, respectively. Also, the results showed that for these deficiently reinforced dapped ends, reducing a/d ratio from 1.5 to 0.75 improved capacity by 23% and 36%. For the deficiently shear-reinforced flanged deep beams, it was found that the inclusion of large openings within the shear span resulted in a capacity drop by (41-49) %. An enhancement of 23% was obtained when using stirrups of 12mm on both sides of the openings. Moreover, it is confirmed that the optimum location of the openings is under the diagonal path. Furthermore, it has been concluded that for loaded openings, the use of T-rolled sections within the bottom chord of the opening yielded an enhancement of 23% relative to the rhombus-shaped configuration.

KEYWORDS: Dapped ends, T-deep beams with openings, Loaded openings, Hanger reinforcement.

INTRODUCTION

Reinforced-concrete structures include a type of regions called (D-regions), at which significant disturbances of stress may occur, resulting in slowing down the stress transfer at these regions (ACI 318, 2019). Consequently, stresses may accumulate in high intensity and then, failure of the structure may be initiated at these regions of unsteady flow of stresses (Lu, 2006; Shakir, 2021; Shakir and Abdel Saheb, 2022). D-regions may be induced due to highly concentrated loads and reactions as in deep beams and corbels, regions of moments and load transfer between members as in beam-column joints, half joints and plie caps or regions at which the path of stress transfer is interrupted or changed severely as in dapped ends (DEs), openings and stepped beams (Aswin, 2015; Shakir, 2020; Zamri et al., 2021). In D-regions, the conventional method of design that is based on Bernoulli formula is not valid to be used (Mattock and Chan, 1979). Two main methods have been proposed in this regard, which are the shear friction (SF) method and the strut and tie model (STM).

Shear friction method was proposed by Mattock and Chan (1979) to consider dapped ends and corbels with shear span/depth (a/d) <1. In 1983, Liem proposed a modified SF method to consider the inclined hanger reinforcement. In 1991, Barton et al. adopted the STM model to simulate DEs with different reinforcement schemes. Yang et al. (2011) proposed a mechanism analysis based on upper-bound theorem to estimate the shear strength of RC DEBs and evaluate the efficiency of the SF method. The results revealed that the PCI SF

Received on 11/5/2022.
Accepted for Publication on 10/8/2022.

design method insufficiently treated the effects of most parameters on the shear strength of DEs. Desnerck et al. (2018) used STM models for dapped ends with corroded steel. Mata-Falcón (2019) proposed a simplified STM to study dapped ends.

More experimental and theoretical studies that mostly adopted STMs were published considering various variables including the concrete strength (Lu et al., 2012; Mohamed et al., 2019), using steel fibre in concrete (Mohammed and Elliot, 2008), shear span/depth ratio (Wang, 2005, Lu, 2015), detailing of dapped ends (Peng, 2009; Mata-Falcon et al., 2019; Shakir and Elliwi, 2020; Shakir and Hamad, 2021), corrosion effect (Desnerck et al., 2018) using internal pre-stressing through dapped ends (Mattock and Theryo, 1986; Botros et al., 2017). Moreover, several proposals have been suggested to improve the performance of deficiently reinforced dapped ends. Such methods included the use of FRP sheets/plates (Huang and Nanni, 2006; Shakir and Abd, 2020), external steel plates (Taher, 2005), external pre-stressing (Atta and Al-Shafeiy, 2014; Atta and Taman, 2016) and NSM steel bars (Shakir and Alliwe, 2021).

Regarding deep beams, STM modeling was adopted widely in evaluating the shear strength of RC deep beams (Dhahir, 2017; Chen, 2018), steel fibre-reinforced concrete deep beams (Lu, 2006; Moradi & Esfahani, 2017), reactive powder concrete deep beams (Fahmi et al., 2013; Hassan, 2015) and hybrid deep beams (Shakir and Hanoon, 2022). Transverse openings may be included to accommodate some services, such as ventilating ducts, heating pipes, sewerage pipes and power cables (Shakir, 2016; Al-Sahlawi, 2018). The ultimate shear strength of a deep beam with openings was calculated using STM model (Shanmugam and Swaddiwudhipong, 1988), regression analysis (Shahnewaz, 2013; Al-khafaji et al., 2014) or genetic algorithm (Shahnewaz and Alam, 2014).

It can be seen that there are several approaches that have been proposed to study the behaviour of D-regions. The SF approach is simple in that application, but limited to a/d<1 and may not consider most of the variables that affect the response. STM models treated all geometries and covered the variables that may affect the behaviour of dapped ends. However, the ideal truss which is the base of the STM method depends on the type of D-region and experience. Mechanism models include many equations to be applied and are limited to specific D-regions, being not general. Regression and genetic algorithm techniques need a huge amount of data.

In this research work, nonlinear finite element analysis has been conducted by using ANSYS software to study the behaviour of deficiently reinforced DEs, T-deep beams with openings and RC beams with loaded openings. A verification study has been presented. Then, a parametric study has been conducted to observe the range of effects of some parameters on the behaviour of such members. The finite element model may be extended to include all types of studies.

Validation Study

The specimens considered in the present work are grouped in three categories of three specimens each. The first group (A) included dapped ends with (a/d) of 1.5, see Fig. (1) (Shakir and Abd, 2020). The width of a specimen was 200 mm. The nib reinforcements for specimens CONT-A, REDH-A (deficient hanger reinforcement) and REDN-A (deficient nib reinforcement) were 2ϕ16, 2ϕ16 and 2ϕ10 mm, respectively. The respective hanger reinforcements were 3ϕ12, 2ϕ10 and 3ϕ12 mm, respectively.

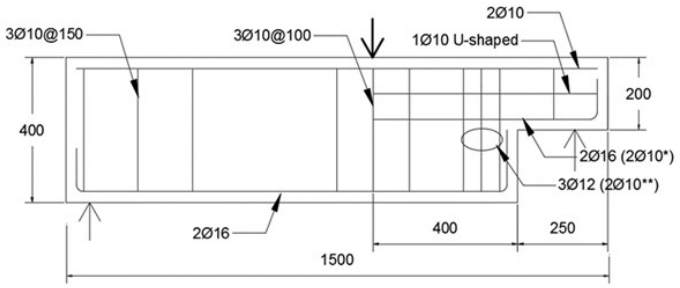

* For reduced nib reinforcement. ** For reduced hanger reinforcement.

Figure (1): Dimensions and detailing of specimens of group A (Shakir and Abd, 2020)

The second group (B) consisted of simply supported T- deep beams, see Fig. (2), with large openings (75 mm height *150 mm width) tested under the effect of two-point loading (Al-Sahlawi, 2018). One of the specimens is solid, the other was 75 mm below the flange, while the other is 75 mm above the bottom of the web. All openings are at (X1=225mm) from the end of the beam. A constant shear span to depth that equals (1.0) was adopted. Longitudinal reinforcements consisted of (3ϕ16) bars and two mesh (10 cm*10 cm- ϕ8mm) bars were used at top and bottom of the flange. No shear reinforcement was used.

The last group consisted of beams with rectangular openings tested under one-point loading within the openings (Hamad & Shakir, 2021). Fig. (3) shows the loading scheme of the dimensions and detailing of strengthening of the openings. The properties for the steel and concrete materials for the three sets are listed in Table 1. Steel plates of 10 mm thickness and 100 mm length with suitable widths (B) according to the width of contact are added at the supports and the point-of-loading positions to avoid the problems of stress concentration. The supporting plates were attached to steel shafts to allow the supports to rotate and move freely. It is to be mentioned that the STM method has been adopted in designing the reference specimen of the three studies.

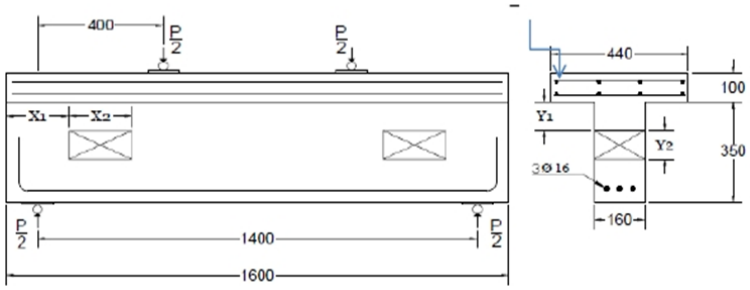

Figure (2): Dimensions and detailing of specimens of group B (Al-Sahlawi, 2018)

Table 1. Material properties for the specimens considered in the present study

Study	Properties			
	Steel			Concrete
	Bar Diameter (mm)	F_y (MPa)	F_u (MPa)	F_{cu} (MPa)
Shakir and Abd	10	568	726	50.53
	12	615	712	
	16	634	748	
Al-Sahlawi	8	509	677	48.5
	18	550	600	
Hamad & Shakir	10	576	674	56
	12	590	684	
	16	600	693	

Nonlinear Finite Element Analysis

The purpose of this section is to check the validation of the finite elements and material models using ANSYS 19.0 software environment to simulate the various D-regions considered in the present work. The validation is fulfilled by comparing load-deflection curves obtained from the analysis with those recorded form experimental tests.

Material Properties

Compressive uni-axial stress-strain behavior has been simulated by an elasto-plastic work hardening model followed by a perfectly plastic response terminated at the onset of crashing, whereas the stress stiffening model has been adopted to represent concrete in tension (Anthony, 2004). The initial modulus of elasticity is used up to the first crack. Then, a smeared crack model is adopted to consider the propagation of cracks. For steel, an elastic behaviour up to the steel yield stress (fy) followed by linear hardening up to the steel ultimate strength (fu) was used. All material models are depicted in Fig. (4).

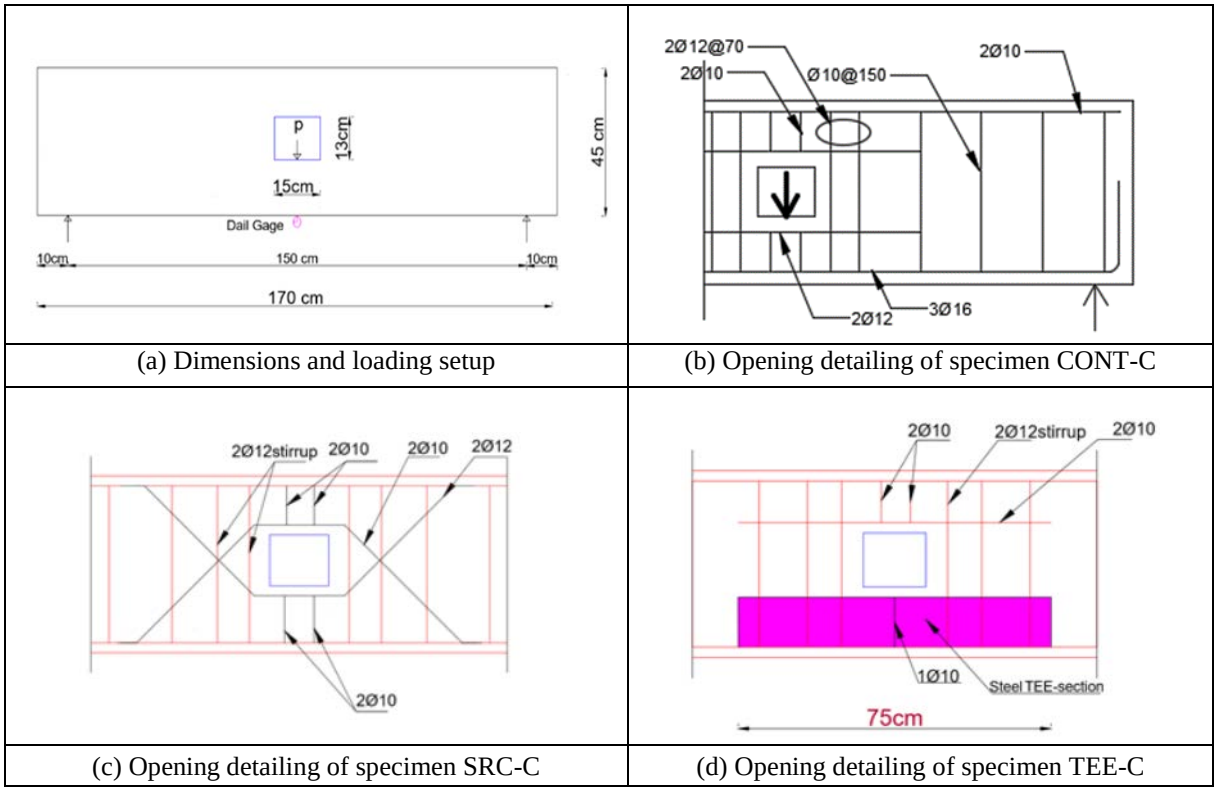

(a) Dimensions and loading setup

(b) Opening detailing of specimen CONT-C

(c) Opening detailing of specimen SRC-C

(d) Opening detailing of specimen TEE-C

Figure (3): Dimensions and detailing of specimens of group C (Hamad & Shakir, 2021)

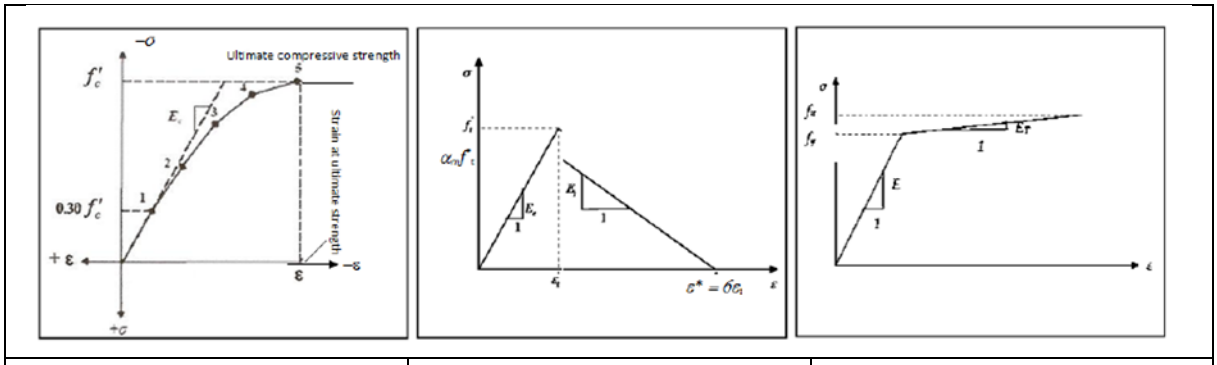

(a) Compression in concrete

(b) tension in concrete

(c) tension in steel

Figure (4): Material models adopted in the present study

FE Modeling

SOLID 65 element is used to model the concrete, because of its ability in accounting for crushing and cracking. SOLID 185 element is used to model the bearing plates. SHELL 181 element is used to model the steel WT-section. Both of the brick elements are defined by eight nodes, while the SHELL 181 is defined by four nodes. LINK 180 element which is defined by two nodes is used to model the steel bars. Each node of the four elements has three degrees of freedom. By taking advantage of symmetry, modeling is carried out making use of the symmetry conditions to minimize modeling and computation time. Figure (5) shows a typical example of meshing. The total distributed load was divided on the nodes so that the share of interior node is twice that of the exterior one. Full bond (no slip) has been proposed between the steel bars/H-shapes and the concrete elements. Regarding the boundary conditions, the roller support is represented by a line of nodes having restrained movement along the Y-axis only. The hinge support is simulated by a line of nodes with degrees of freedom restrained in X-and Y-directions.

The plane of symmetry has been represented by nodes with degrees of freedom restrained in the direction perpendicular to the plane of symmetry only.

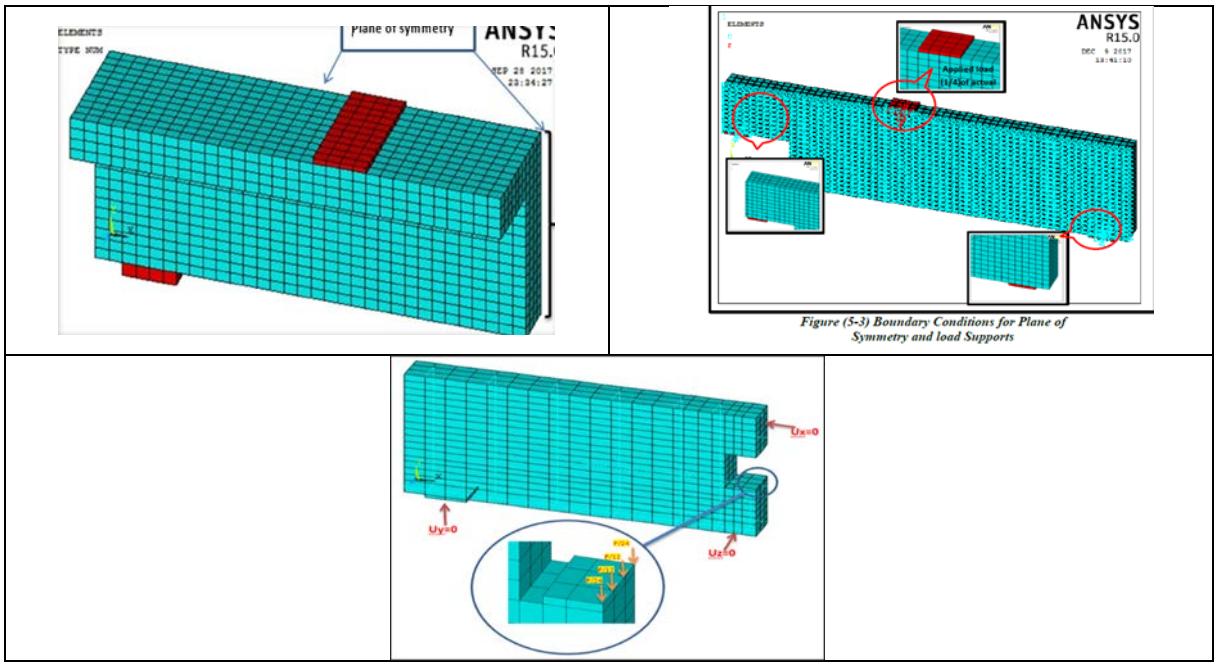

Figure (5): Modeling of the tested specimens making use of symmetry

DISCUSSION OF RESULTS

Fig. (6a) shows a comparison between the experimental and theoretical results for the specimens of group A. It can be observed that the numerical results yielded a stiffer response than the corresponding experimental ones. This may be due to the material models which may not simulate the materials exactly, full-bond assumption, … etc.

However, the differences in failure load and deflection at failure are very slight. It can be seen that reducing hanger reinforcement by 25% reduced capacity by 15%. The same reduction in nib reinforcement reduced capacity by 32%. This reveals that the beam is more prone to failure when the nib reinforcement is reduced due to the higher disturbance of stresses and the smaller depth of the section. Consequently, the beam may fail rapidly by diagonal shear from the re-entrant corner or by flexural failure. Thus, it is important to put in mind that the extended end is not to be designed as a cantilever beam which may result in inefficient transfer of stresses away from the re-entrant corner.

For the specimen with reduced hanger reinforcement, the reduction has been observed to be 20% of that corresponding to the nib reduction. This may be attributed to that the region attached to the extended end is less disturbed than the junction region and that the smaller amount of stirrups may resist the tensile stresses more adequately than the reinforcement of the nib end. This may be due to that the section of concrete with the hanger reinforcement may resist the shear stresses. Also, the legs of the hanger stirrups resisted the tensile stresses beyond the limited value (420 MPa) up to failure. The results showed also that there is some stiffening in the finite elements within the early stages of loading near the cracking loads due to reasons discussed previously. Thus, the sensitivity to the change in geometry close to the cracking stage is relatively small. Then, the stresses are resisted by the steel crossing the junction interface, leading to a new mechanism that controls the behaviour up to failure. Good agreement between the finite element analysis results and experimental results can be observed.

Fig.(6b) shows a comparison between the FE analysis results and the experimental ones for group B. It can be seen that there is a relatively better agreement

between the results of the three specimens throughout most of the loading history. However, there is a small lack in the predicted defection at failure. This may be attributed to that less disturbance may exist with the T-deep beams compared to the dapped ends. Also, it can be seen that introducing the opening in contact with the flange reduced capacity by 43%, while making the opening near the tension face reduced capacity by 49%. It can be observed that locating the opening close to the flange did not control failure significantly and the opening may be shifted out of the path of the diagonal crack. Moreover, it can be observed that locating the opening within the shear zone and on the line matching the concentrated load with the support point (bottom location) with no stirrups around the opening may resist vertical tension and separation at a horizontal plane through the opening.

Fig.(6c) shows the load-deflection curves for group C. As usual, FE analysis results showed a slightly stiffer response than the experimental results. Furthermore, it can be observed that the specimen with the opening strengthened by the TEE-steel section yielded the highest capacity due to the efficiency in transferring the stress induced by the concentrated load to the largest regions around the opening. The specimen in which the opening is with a rhombus-shaped steel bar-reinforcement showed the lowest capacity, because only the V-shaped bars work effectively against cracking emanating from the corners of the opening and the tensile forces on both sides of the opening are resisted by the vertical component only.

It can be concluded from the above discussion that the finite-element and the material models adopted in the present study are adequate to simulate various types of D-regions. In general, good agreement has been obtained for most of the loading history with some stiff behaviour within the cracking-load stage. Similar failure loads have been obtained with a very slight lack in the corresponding deflection.

Parametric Studies

Dapped-end Beam

For the control specimen, Fig. (7a), CONT-A, it can be observed that reducing a/d from 1.5 to 1.0 resulted in an improvement in failure load by 13%. Reducing a/d to 0.75 led to an enhancement in capacity by 10%. The corresponding reductions in maximum deflection were 19% and 50%, respectively. The reduction of capacity at a/d=0.75 may be attributed to transferring the failure to another mode. It can be observed that reducing a/d resulted in shifting the failure to occur within the full-depth beam (hanger region), due to enhancement in rigidity. Thus, the recorded deflection reduced, stiffness increased, capacity increased, but toughness reduced. It can be concluded that adopting a smaller value of a/d for adequately reinforced dapped ends may result in load-capacity and stiffness enhancement, while reductions in ductility and toughness nay be obtained.

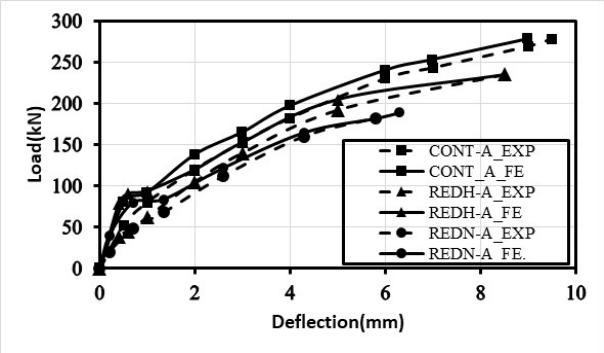

a) Group A

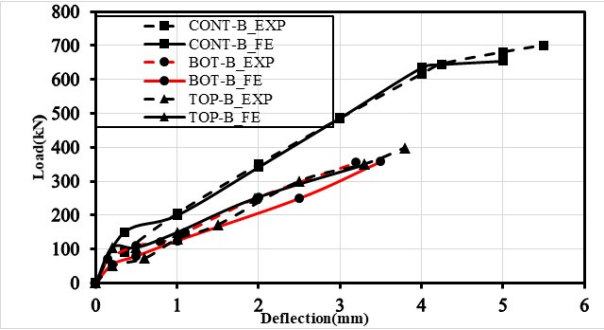

B) Group B

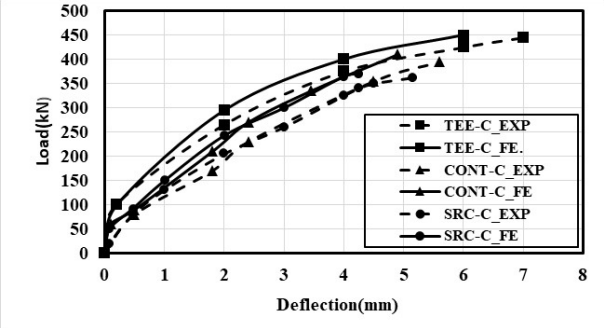

C) Group C

Figure (6): Load-deflection curves for the tested specimens

For specimen REDH-A, Fig.(7b), it is clear that reducing a/d ratio from 1.5 to 0.75 resulted in enhancing

failure load by 23% and deflection at failure reduced by 45%. It can be observed that the dapped end tends to follow the same behavior as the fully reinforced dapped end when reducing a/d value with a smaller capacity, less stiffness and higher deflection. This is because of the relatively smaller rigidity compared to the fully reinforced dapped end. Thus, it can be concluded that stiffness may be enhanced gradually with a/d reduction. However, toughness and cracking ductility are expected to be reduced accordingly.

For the deficiently nib end specimen REDN-A, Fig.(7c), it is clear that reducing a/d ratio to 0.75 enhanced failure load by 36% and the maximum deflection increased by 40%. For such deficient ends, the weakness in nib end is controlled by reducing a/d ratio (reducing the effect of bending moment). Then, for high values of a/d, failure occurred at early stages by flexure with a relatively small deflection at failure. When reducing a/d value, the effect of B.M. reduced. Thus, sudden failure by flexure at nib end is controlled to some limit. For a/d=0.75, the strength of nib end may become enough. Consequently, rigidity increased and maximum deflection reduced. Significant increases in ductility, toughness and stiffness may be obtained.

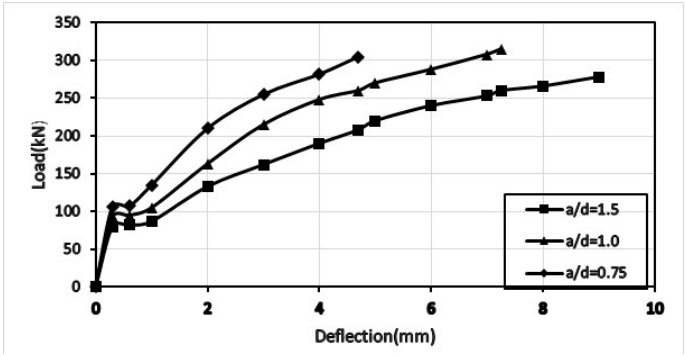

a) Specimen CONT-A

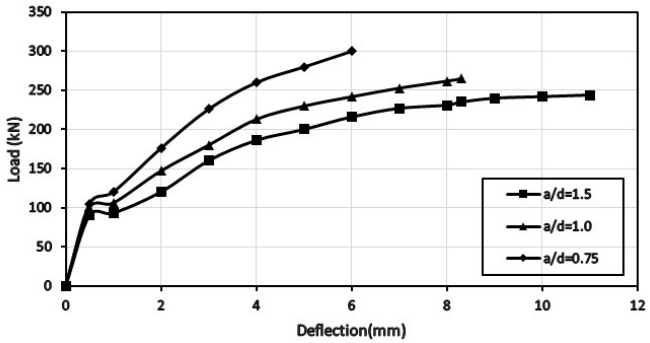

b) Specimen REDH-A

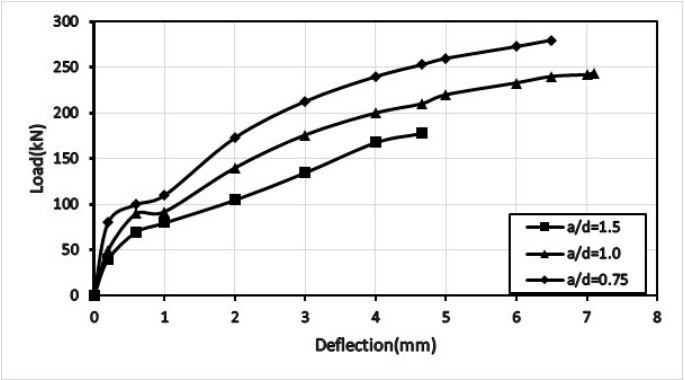

c) Specimen REDN-A

Figure (7): Effect of (a/d) ratio on the behavior of the specimens of group A

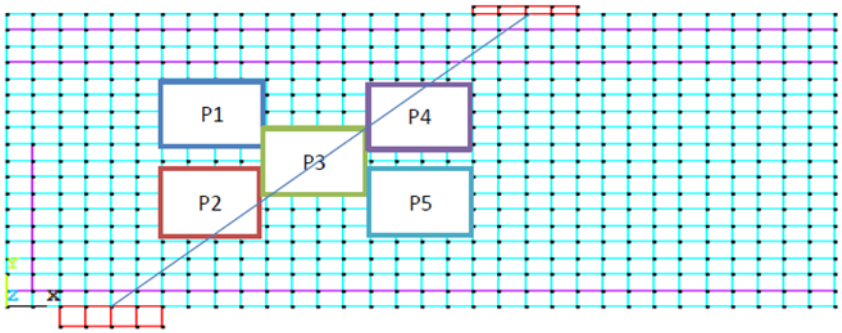

Figure (8): The possible location of openings within the shear span

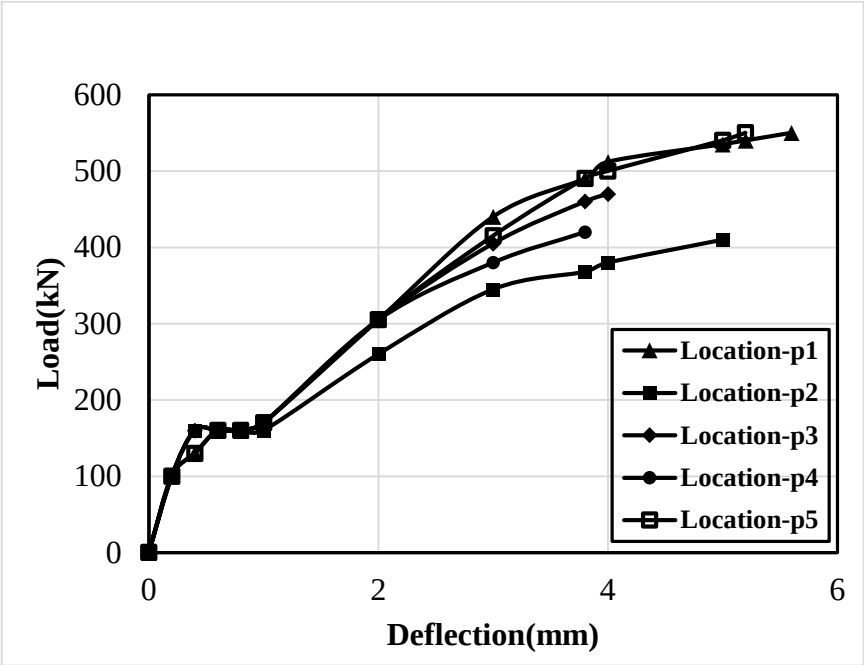

Figure (9): Load-deflection curves for the T-beam with different opening locations

T-deep Beams

The location of the opening with respect to the line of diagonal shear is discussed. Five locations are considered, see Fig. (8). It is clear from Fig. (9) that locating the openings out of the diagonal line (location P1) yielded the optimum response with 545 kN. This may be attributed to that the corner is considered as a dead region.

For location P5 (maximum bending moment), flexural cracking may be initiated at the corners of the openings within this stage. For location P2, there is a combined effect of stresses. Severe crushing may be developed due to bearing stresses near support and diagonal shear stresses. Thus, it can be seen that this location yielded the lowest load capacity (411 kN).

For location P4, also two effects may be induced; one is that some crushing may occur due to excessive compressive stresses and the other is due to diagonal cracking. However, crushing occurs at the final stages of loading, resulting in a stiffer response with less ductility.

For location P3, it can be seen that the opening is located at the mid- point on the diagonal line. Then, crushing effects may not reach the opening up to the final stages, resulting in stiffness and capacity enhancements.

Fig. (10) shows the effect of vertical stirrups around the openings of specimen TOP-B. It is clear that there is no significant effect on capacity for a diameter of 8 mm. This may be attributed to that the small tensile area may not provide efficient strength to the horizontal separation. Increasing the diameter of the stirrups to 12mm, tensile resistance increased, resulting in a delay

of horizontal separation, providing more shear resistance to diagonal cracking and providing the dowel action efficiently.

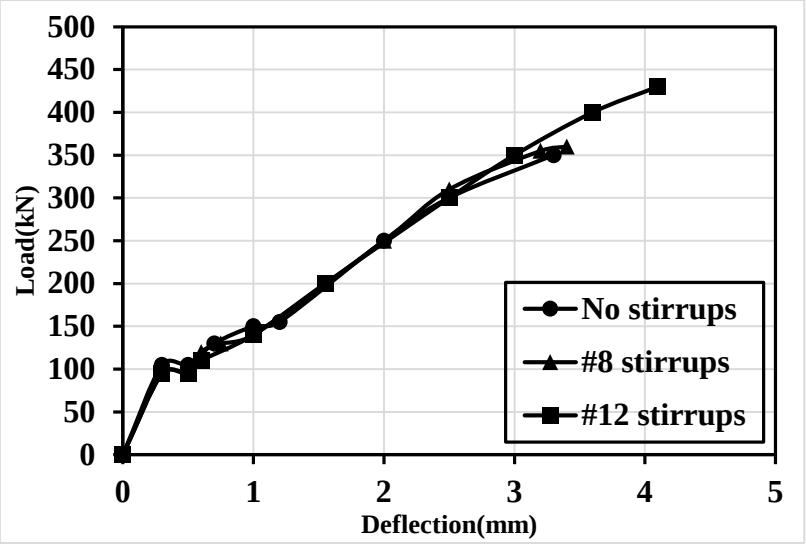

Figure (10): Effect of using stirrup reinforcement on both sides of the opening

CONCLUSIONS

1. The finite-element and material models adopted in the present work predicated adequately the behaviour of the RC beam including severely stressed regions. Moreover, the effect of deficiencies in design can be predicted efficiently. The same models can be used for different D-regions compared to the STM models that need to be formulated for each case.
2. For dapped ends, deficiently designed hanger or nib reinforcement by 25% resulted in reductions of capacity by 15% and 32%, respectively. Thus, great attention should be given to the design of nib reinforcement.
3. The shear span/depth ratio has a dominant effect on the response of dapped ends, especially those including deficient nib reinforcement. It was found that reducing the ratio from 1.5 to 0.70 improved that capacity by 10%. For 25% deficient nib reinforcement, the improvement was 57%. The respective enhancement for hanger reinforcement was 23%.
4. Inclusion of large openings within the shear span of deficiently shear- reinforced T-deep beams reduced the load capacity by a range of (41-49) % depending on the location of the openings.
5. For flanged deep beams, the optimum location of openings is flush to the flange and out of the diagonal cracking path. The enhancement in capacity was obtained to be 32% relative to the location within the diagonal path and close to the supports.
6. The behaviour of deficiently reinforced T-deep beams with large openings may be improved by using some reinforcement on both sides of the openings in the form of NSM steel bars or CFRP wrapping. The results revealed that using stirrups of 12mm improved the capacity by 23% relative to the case of no shear reinforcement.
7. Using vertical stirrups on both sides of a loaded opening yielded better response than using a rhombus- shaped reinforcement around the opening. Also, using a T-rolled section within the bottom chord improved the capacity by 23% relative to the case with rhombus reinforcement.
8. The present finite-element and material models may be extended to more D-regions as corbels, inverted T-beams, pile caps, beam-column joints, … etc.

REFERENCES

ACI CODE-318-19. "Building code requirements for structural concrete". American Concrete Institute (ACI), Farmington Hills, Mich., 623 pp.

Al-Khafaji, J., Al-Shaarbaf, I., and Sultan, W.H. (2014). "Shear behavior of fibrous self-compacting concrete deep beams". Journal of Engineering and Development, 18 (6), 36-58.

Al-Sahlawi, Y.M. (2018). "Strengthening of self-compacting reinforced concrete t-deep beams with openings by CFRP sheets". MSc Thesis, University of Kufa, Iraq, 104pp.

Aswin, M., Mohammed, B.S., Liew M.S., and Syed, Z.I. (2015). "Shear failure of RC dapped-end beams". Hindawi Publishing Corporation Advances in Materials Science and Engineering, 1-10.

Atta, A., and Taman, M. (2016). "Innovative method for strengthening dapped-end beams using an external pre-stressing technique". Materials and Structures, 49 (8), 3005-3019.

Atta, A.M., and Al-Shafiey, T.F. (2014). "Strengthening of RC dapped end beams under torsional moments". Magazine of Concrete Research, 66 (20), 1065-1072.

Barton, D.L., Anderson, R.B., Bouadi, A., Jirsa, J.O., and Breen, J.E. (1991). "An investigation of strut-and-tie models for dapped beam details". Research Report, Number, 1127-1,187pp.

Botros, A.W, Klein, G.J., Lucier, G.W., Rizkalla, S.H., and Zia, P. (2017). "Dapped ends of prestressed concrete thin-stemmed members- Part 1: Experimental testing and behavior". PCI Journal, March-April.

Chen, H., Yi, W.-J., and Hwang, H.-J. (2108). "Cracking strut-and-tie model for shear-strength evaluation of reinforced concrete deep beams". Engineering Structures, 163, 396-408.

Desnerck, P., Lees, J.M., and Morley C.T. (2018). "Strut-and-tie models for deteriorated reinforced concrete half-joints". Engineering Structures, 161, 41-54.

Desnerck, P., Lees, J.M., and Morley, C.T. (2018). "Strut-and-tie models for deteriorated reinforced concrete half-joints". Engineering Structures, 161, 41-54.

Dhahir, M.K. (2017). "Shear strength of FRP-reinforced deep beams without web reinforcement". Composite Structures, 165, 223-232.

Fahmi, H.M., AlShaarbaf, I.A.S., and Ahmed, A.S. (2013). "Behavior of reactive powder concrete deep beams". Al-Mansour Journal, 20, 1-22.

Hamad, S.A., and Shakir, Q.M. (2021). "Behaviour of RC beams with strengthened web openings under vertical loads". IOP Conf. Ser. Mater. Sci. Eng., 1094 (1), 012062, doi: 10.1088/1757-899x/1094/1/012062

Hassan, H.F. (2015). "Behavior of hybrid deep beams containing ultra-high-performance and conventional concretes". Eng. & Tech. Journal, 33 (1), Part (A).

Huang, P.C., and Nanni, A. (2006). "Dapped-end strengthening of full-scale prestressed double tee beams with FRP composites". Advances in Structural Engineering, 9 (2), 293-308.

Liem, S.K. (1983). "Maximum shear strength of dappedend or corbel". M.Sc. Thesis, Concordia University, Montreal, Quebec, Canada, 127p.

Lu, W.-Y. (2006). "Shear strength prediction for steel-reinforced concrete deep beams". Journal of Constructional Steel Research, 62, 933-942.

Lu, W.-Y., Chen T.-C., and Lin, I.-J. (2015). "Shear strength of reinforced concrete dapped-end beams with shear span-to-depth ratios larger than unity". Journal of Marine Science and Technology, 23 (4), 431-442.

Lu, W.Y., Lin, I.J., and Yu, H.W. (2012). "Behaviour of reinforced concrete dapped-end beams". Magazine of Concrete Research, 64 (9), 793-805.

Mata-Falcón, J., Pallarés, L., and Miguel, P.F. (2019). "Proposal and experimental validation of simplified strut-and-tie models on dapped-end beams". Engineering Structures, 183, 594-609.

Mattock, A.H., and Chan, T.C. (1979). "Design and behavior of dapped-end beams". PCI Journal, November-December, 28-45.

Mattock, A.H., and Theryo, T.S. (1986). "Strength of precast prestressed concrete members with dapped ends". PCI Journal, 31 (5), 58-75.

Mohamed, R.N., and Elliott, K.S. (2008). "Shear strength of short recess precast dapped-end beams made of steel fibre-self-compacting concrete". 33rd Conference on Our World in Concrete & Structures, 25-27 August, Singapore.

Mohammed, B.S., Aswin, M., Liew, M.S., and Zawawi, N. (2019). "Structural performance of RC and R-ECC dapped-end beams based on the role of hanger or diagonal reinforcements combined by ECC. Int. J. Concr. Struct. Mater., 13 (44).

Moradi, M., and Esfahani, M.R. (2017). "Application of the strut-and-tie method for steel fiber reinforced concrete deep beams". Construction and Building Materials, 131, 423-437.

Peng, T. (2009). "Influence of detailing on response of dapped-end beams". McGill University, Montréal, Canada.103p.

Shahnewaz, Md. (2013). "Shear behavior of reinforced concrete deep beams under static and dynamic loads". Master Thesis of Applied Sciences, University of British Columbia, (Okanagan), 124pp.

Shahnewaz, Md., and Alam, M.S. (2014). "Improved shear equations for steel fiber-reinforced concrete deep and slender beams". ACI Structural Journal, 111(1-6), 1-10.

Shakir, Q. M., and Alliwe, R. (2020). "Upgrading of deficient disturbed regions in precast RC beams with near-surface mounted (NSM) steel bars". Journal of Materials and Engineering Structures, 7 (2), 167-184.

Shakir, Q.M. (2016). "Non-linear analysis of high-strength reinforced concrete beams with large openings". Jordan Journal of Civil Engineering, 10 (4): 451-461.

Shakir, Q.M. (2020). "A review on structural behavior, analysis and design of RC dapped-end beams". 3rd International Conference on Recent Innovations in Engineering (ICRIE 2020), IOP Conf. Series: Materials Science and Engineering, 978 012003.

Shakir, Q.M. (2021). "Behavior of high-performance RC composite corbels with inclined stirrups". Canadian Journal of Civil Engineering, 12 (1). https://doi.org/ 10.1139/cjce-2020-0149.

Shakir, Q.M., and Abd, B.B. (2020). "Retrofitting of self-compacting RC half joints with internal deficiencies by CFRP Fabrics". Jurnal Teknologi, 82 (6), 49-62.

Shakir, Q.M., and Abdlsaheb, S.D. (2022)." Rehabilitation of partially damaged high-strength RC corbels by EB FRP composites and NSM steel bars". Structures, 38 (2), 652-671. doi: 10.1016/j.istruc.2022.02.023.

Shakir, Q.M., and Alliwe, R. (2021). "Behavior of high-strength self-compacting reinforced concrete corbels strengthened with NSM steel bars". Int. J. Adv. Sci. Eng. Inf. Technol., 11 (2), 663-673. https://doi.org/ 10.18517/ijaseit.11.2.8059

Shakir, Q.M., and Hamad, S.A. (2021). "Behavior of pocket-type high-strength RC beams without or with dapped ends". Pract. Period. Struct. Des. Constr., 26 (4), 1-12.

Shakir, Q.M., and Hanoon, H.K. (2022). "Behaviour of high-performance reinforced-concrete hybrid deep beams". Journal of Engineering Science and Technology, 17 (6).

Shanmugam, N.E., and Waddiwudhipong, S.S. (1988). "Strength of fibre-reinforced-concrete deep beams containing openings". The Interactional Journal of Cement Composites and Light-weight Concrete, 10 (1), 53-60.

Taher, S.F. (2005). "Strengthening of critically designed girders with dapped ends". Structures & Buildings, 158 (2), 141-152.

Wang, Q., Guo, Z., and Hoogenboom, P.C.J. (2005). "Experimental investigation on the shear capacity of RC dapped-end beams and design recommendations". Structural Engineering and Mechanics, 21 (2), 221-235.

Yang, K.-H., Ashour, A.F., and. Lee, J.-K. (2011). "Shear strength of reinforced concrete dapped-end beams using mechanism analysis". The University of Bradford Institutional Repository, 1-38.

Zamri, N.F., Mohamed, R.N., and Elliott, K.S. (2022). "Shear capacity of precast half-joint beams with steel fibre-reinforced self-compacting concrete". Construction and Building Materials, 272, 1-12.